J Braz. Soc. Mech. Sci. Eng.
DOI 10.1007/s40430-016-0538-2

TECHNICAL PAPER

Energy conservation for refrigeration systems by means of hybrid fuzzy adaptive control techniques

Enio Pedone Bandarra Filho[1] · Oscar Saul Hernandez Mendoza[1] · Francisco Ernesto Moreno Garcia[2] · Jose Alberto Reis Parise[3]

Received: 23 October 2015 / Accepted: 1 April 2016

Abstract Most vapour compression refrigeration systems still operate under on–off control, although it is well known that the application of any other control method could result in improved COP. For that purpose, the present paper experimentally studies the use of adaptive fuzzy hybrid control and design of experiments techniques, as well as the application of the response surface methodology, in a 5-ton vapour compression system with a variable speed compressor and an electronic expansion valve. Evaporation temperature and evaporator overall conductance were found to be the most relevant input parameters to the fuzzy hybrid control system, where the optimal trajectory was sought without taking into account the elapsed time. Results have shown that the knowledge of the most relevant parameter of the system allowed for the control system to seek high COP zones. It has been found that this type of technique does not jeopardize the control performance, which remains robust.

Keywords Refrigeration system · Control · Fuzzy adaptive · Fuzzy hybrid · Coefficient of performance

Technical Editor: Francis HR Franca.

✉ Enio Pedone Bandarra Filho
bandarra@ufu.br

Oscar Saul Hernandez Mendoza
oscarshm5@gmail.com

Francisco Ernesto Moreno Garcia
femgarcia@ufps.edu.co

Jose Alberto Reis Parise
parise@puc-rio.br

[1] School of Mechanical Engineering, Federal University of Uberlandia, Av. Joao Naves de Avila, 2121, Santa Monica, Uberlandia, MG 38400-902, Brazil

[2] Engineering Department, Universidad Francisco de Paula Santander, Avenida Gran Colombia No. 12E-96, San Jose de Cucuta, NS, Colombia

[3] Department of Mechanical Engineering, Pontifícia Universidade Católica do Rio de Janeiro, Rua Marques de Sao Vicente, 225, Gavea, Rio de Janeiro, RJ 22451-900, Brazil

List of symbols

Symbols

A	Scheme of the control related to the number of steps of the EEV
B	Scheme of the control related to the compressor speed
COP	Coefficient of performance (–)
$e(k)$	Inlet error of the adaptive fuzzy PI control (A)
$ea(k)$	Accumulated inlet error of the fuzzy PI control (A)
$\Delta e(k)$	Change in inlet error of the adaptive fuzzy PD control (B)
Δe	Mean absolute change in inlet error of the adaptive fuzzy PD control (B)
f_e(k)	Estimated frequency (Hz)
f_r(k)	Real frequency (Hz)
FREQ	Frequency of compressor (Hz)
IAE	Integral of the absolute error value
ITAE	Integral of the absolute error value time weighted
k	Refer to instant of time
KKv	Adaptive mechanism of internal factor of the adaptive fuzzy PD control (B)
k_{pc}	Gain of the fuzzy PI control (A)
Kv	Sensibility scale factor of the adaptive fuzzy PD control (B)
N	Negative set of the adaptive fuzzy PD control (B)

Published online: 16 April 2016

$\dot{m}_{r22}$	Refrigerant mass flow rate (kg/s)
NEEV	Number of steps of the electronic expansion valve (–)
R	Positive set of the adaptive fuzzy PD control (B)
P_1	Compressor suction pressure (kPa)
P_2	Compressor discharge pressure (kPa)
P_3	Condensation pressure (kPa)
P_4	Pressure measured downstream the electronic expansion valve (kPa)
$\dot{Q}_{ev}$	Cooling capacity (kW)
Δt	Period of time (s)
t_a	Settlement time period (s)
T_{cd}	Condensation temperature (°C)
T_{ev}	Evaporation temperature (°C)
T_1	Refrigerant temperature at the evaporator outlet (°C)
T_5	Water temperature at the evaporator outlet (°C)
T_8	Water temperature at the evaporator inlet (°C)
ΔT_{sc}	Degree of subcooling (°C)
ΔT_{sh}	Degree of superheat (°C)
UA	Heat exchanger conductance (kW/m^2 K)
U_c	Output signal of the fuzzy adaptive PD controller (B)
U_k	Output signal of the fuzzy PI controller (A)
U_2	Output signal to the actuator of the fuzzy PI controller (A)
$\|Uc\|$	Mean absolute exit signal of the fuzzy adaptive PI control (B)
$u(e)$	Pertinence function inlet error of the adaptive fuzzy PI control (A)
$u(ea)$	Pertinence function inlet error accumulated of the adaptive fuzzy PI control
UA	Heat exchanger overall conductance (kW/K)
$\dot{W}$	Power consumption (kW)
Z	Zero set of the adaptive fuzzy PD control (B)

Abbreviation

CCF	Central composite design—face centred
DOE	Design of experiments
EEV	Electronic expansion valve
FET	Field effect transistor
LN	Mean large negative
LP	Large positive
MN	Medium negative
MP	Medium positive
MSR	Methodology of response surface
N	Negative
P	Positive
PID	Proportional integral derivative controller
PLC	Programmable logic controller
QQR	Optimal lineal quadratic control
SISO	Traditional control for one entrance and one exit
SN	Small negative
SP	Small positive
TXV	Thermostatic expansion valve
Z, ZO	Zero

1 Introduction

Conventional refrigeration and air conditioning systems are usually designed to meet the maximum cooling load. However, given the significant variation in load conditions that may occur, these systems operate much of the time at partial load or in transient regime. The operation at partial load is normally tackled using on/off control of the compressor or, less frequently, with PID control. The combination of control acting on the variable speed compressor and the electronic expansion valve has been regarded in the literature as a more efficient way of managing the operation of a vapour compression cycle [16]. For instance, Bandarra Filho et al. [3] showed that auto tuning PID control presented better results than the classical PID, and that feedback control is only used in case of systems with slow response, where it becomes necessary to know the system model, either obtained through the manufacturer catalogue or experimentally. Shunagquan [23], Koury et al. [14] and Vargas and Parise [27] reported improvements of up to 11 % in energy efficiency by replacing the on–off system with a variable speed compressor, due to better control of the evaporation temperature and, consequently, of the cooling capacity. Schurt et al. [24] proposed a MIMO controller based on the Linear-Quadratic-Gaussian technique. They found the controller maintained the refrigeration system for small capacity running properly and that the controller performed well not only for reference tracking, but also for disturbance rejection. Oliveira et al. [19] proposed a switching control strategy for small-capacity vapour compressor refrigeration systems and concluded the controller has shown to be able to drive the system toward the reference rapidly.

In spite of emerging technologies, the fundamental task for the vapour compression cycles, generally used in air conditioning systems, is to control, in a safe and reliable form, the air temperature (and, sometimes, relative humidity) in the refrigerated ambient. This can be accomplished by the variation of compressor capacity (on/off or variable speed operation) and by proper operation of the thermostatic expansion valve (TXV). For its ability to control the degree of superheat at the evaporator outlet, providing effective use of the heat exchanger throughout its entire length, the TXV has proved to be a suitable expansion device, ensuring the safety of compressor operation, even for systems with wide variations in the refrigeration load [8]. In this respect, Dhar and Soedel [7], as well as Lenger et al. [15], examined the influence of a conventional

TXV on the stability of the system. Higuchi and Hayano [11] established a transfer function for the flow response by means of the TXV.

Mithraratne and Wijeysundera [17] studied the dynamic behaviour of a TXV controlled dry evaporator. They concluded that the amplitude and frequency of observed hunting oscillations depended on: the superheating setting, evaporator heat load and TXV time constant. Chen et al. [6] presented an overview on former studies on the stability of TXV-controlled refrigeration systems. Two possible explanations for the hunting behaviour of TXV-evaporator systems were drawn from their review: it is caused by the evaporator characteristics or by the stability of the evaporator fluid supply control system.

In summary, the above-mentioned authors focused their studies on the expansion device and the evaporator, in order to improve the efficiency of refrigeration and air conditioning systems.

To a certain extent, TXV control fails to satisfy some of the needs of HVAC&R systems, particularly with severe thermal load transients [22], giving way to electronic expansion valves (EEV), which have been increasing their application in this area. Similarly, concerning the stability of EEV systems, studies are guided by two aspects: system characteristics and operation. Outtagarts et al. [20] performed an experimental study by varying the refrigerant flow using EEV. The response of the evaporator, time constant and lags were identified as a function where evaporator temperature and compressor speed were key parameters. Jia et al. [12] observed the operation of a refrigeration system in small transitional periods, by slightly decreasing or increasing the flow of refrigerant. It was concluded that, with a simple PID control, one could meet satisfactorily the operation of the system without being concerned with the path followed by the control. Yasuda [28] studied the relationship between parameters of stable operation of the refrigeration system and had, as results, inlet and outlet refrigerant temperatures of the evaporator for different expansion valve positions. In addition, Yasuda [28] developed two transfer functions to control the system, and also showed the effect of PI control parameters on system stability, noting that, for high values of proportional and integral constants (PI), the EEV controller tends to prolong the time to stabilize the system (time path followed by chaotic and slow control).

A number of applications dealing with fuzzy control applied to refrigeration systems have been conducted, reporting considerable energy savings when compared to conventional controllers (for example, [2, 9, 13, 26]. Fuzzy logic is becoming a usual resource in advanced designs of controllers due to, predominantly, the qualitative description involved in the controller. In that respect, fuzzy logic can play the same role as a mathematical equation in the conventional control theory. Ekren et al. [10] performed a comparative study among three different control strategies, including PID, fuzzy logic and artificial neural network. They concluded that the artificial neural network achieved the lowest power consumption, of 8.1 and 6.6 %, in comparison to PID and fuzzy logic controls, respectively. Bandarra Filho et al. [3] conducted an experimental study using adaptive control in a refrigeration system, composed by a semi-hermetic compressor, "tube-in-tube" condenser and evaporator, and TXV. Tests were performed with a variable speed compressor in the range of 30–70 Hz. The experimental results showed that the highest coefficient of performance (COP) was attained by working in the range of 50 Hz, using adaptive fuzzy control technique. The adaptive fuzzy control technique, applied to modulate the compressor speed, enabled a reduction in energy consumption of the order of 17.8 %, in comparison with the on–off control. Pinolla et al. [21] performed an experimental study based on an alternative solution for reducing the energy consumption in refrigeration systems. The authors found a reduction on energy consumption of up to 31 % when the system operated for about 6 h. Beyond this, the compressor cycling frequency was also reduced in comparison with the traditional on–off system.

The encouraging results reported above, as far as energy consumption is concerned, for adaptive control applied to refrigeration systems, pave the way for further research. The objective is to find a control algorithm for the vapour compression refrigeration system with improved performance for a given cooling capacity. This paper presents an experimental application of different control techniques to run efficiently a 5-ton vapour compression refrigeration system, by controlling the degree of superheat and compressor speed, aiming at the highest COP value for a prescribed set point. To the authors´ knowledge, no other work with similar approach, i.e., the use of adaptive fuzzy hybrid control and design of experiments techniques, as well as the application of the response surface methodology, has been found to date in the open literature.

2 Experimental apparatus

The test rig used for data collection is composed of two circuits: a secondary water loop and a primary refrigerant circuit. Figure 1 shows schematically the test facility. Refrigerant (R22) flow is provided by a semi-hermetic compressor. The evaporator, with a cooling capacity of 17.5 kW (5-ton), is a "tube-in-tube" heat exchanger where refrigerant flows inside the central tube and water, through the annular space. To ensure the compressor integrity, a liquid separator was installed to avoid the possibility of liquid slug. A "tube-in-tube" condenser, of the same

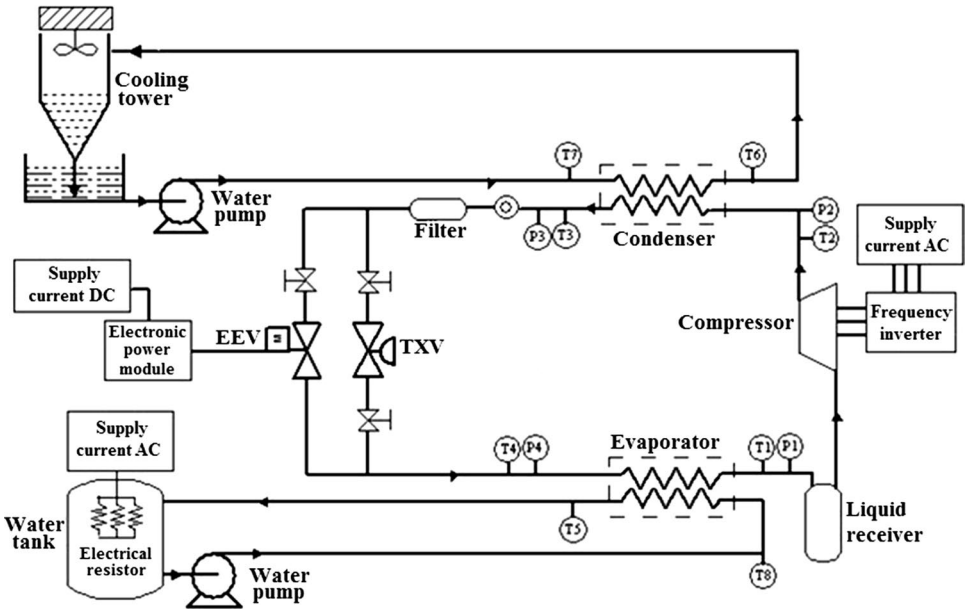

Fig. 1 Schematic view of the experimental facility

nominal capacity as the evaporator, was used. The two heat exchangers were thermally insulated, in order to minimize heat exchange with the environment. A cooling tower was used for the heat rejection of the condenser cooling water. The evaporator water, the secondary fluid, responsible for the variation of the thermal load of the system, was supplied from an isolated tank of 50 l. An electric resistance of 15 kW was installed in this tank, in order to maintain the evaporator water inlet temperature at 20 °C. Piezoresistive sensors were used to measure pressures, and PT100 sensors, for temperatures. A frequency inverter was used to control and measure the speed of the compressor. A Coriolis-type mass flow meter recorded refrigerant mass flow rate.

Data acquisition was carried out by means of an electronic board with analogue output signal. The analogue signals were converted to digital signals through a programmable logic controller (PLC). Data were then monitored and managed by a program written in the LabVIEW platform. The system had installed a TXV with a nominal capacity of 5-ton, as shown in Fig. 1. An EEV, operated by a bipolar motor, was installed in parallel with the TXV. The accuracy of the measurements was determined according to the procedure suggested by Abernethy and Thompson [1], with a confidence interval of 95 %, as shown in Table 1.

Table 1 Uncertainty of the measured parameters

Parameter	Type	Accuracy
Temperature	Measured	±0.15 K
Pressure	Measured	±0.30 %
Mass flow rate	Measured	±0.15 %
Power consumption	Measured	±0.037 kW
Cooling capacity	Propagated	±5.62 %
COP	Propagated	±6.43 %

3 Refrigeration system modelling

To obtain knowledge of the dynamic behaviour of the controlled variables, the refrigeration system was subjected to a series of experimental runs, planned from a design of experiments (DOE) application, which defined the data to be collected, namely, number of runs and operational conditions. The trends of system parameters in response surfaces were analysed assuming quasi-steady-state conditions. There are two main types of experimental arrangements for data collection, based on the response surface methodology: the central composite design of experiments and the Box–Behnken design, Box et al. [5]. A face-centred central composite design (FCCCD), characterized by having points on the axial centre of each face of the space factor, i.e., $\alpha = +1$ or $\alpha = -1$, was applied. Three levels for each factor are required. The two factors acting in the system, number of steps of the electronic expansion valve (NEEV) and the compressor frequency (FREQ), were used and the controlled variables were defined with maximum $(+1)$ and minimum (-1) values, called levels. These levels were correlated to a central reference level (level 0), as shown in Table 2.

Expansion valve steps and compressor frequency were then used as factors of the experimental plan, requiring 12 randomized trials, with four replicates at the central point

Table 2 Factors and adopted levels used in experimental planning CCF

Expansion valve steps			Compressor frequency		
VEE (steps)			FREQ (Hz)		
Factors					
−1	0	+1	−1	0	+1
−α		+α	−α		+α
−400	0	+400	40	50	60
Opening ←	Closing →		Lower frequencies ←		Higher frequencies →

for estimation of the experimental error. The combination of the responses resulted in a multi-variable correlation (linear or quadratic model), which facilitated understanding and visualizing the behaviour of the process controlled variables, namely: evaporating temperature, refrigerant mass flow rate, cycle coefficient of performance, condensing temperature, cooling capacity and power consumption.

According to Myers and Montgomery [18], the response surface methodology (RSM) is a combination of mathematical and statistical techniques that are used to model and analyse problems in which the response of interest is influenced by a number of controlled variables.

According to Box et al. [4], almost all response surface problems use models of the first or second order. Furthermore, it is unlikely that a single polynomial model is a reasonable approximation to the actual model over the entire experimental domain. On the other hand, at least for a certain region, it might work well, according to Myers and Montgomery [18].

The resulting behaviour of refrigerant mass flow rate and evaporation temperature could be represented by the following objective functions:

$$m_{r22} = 0.0162 + 5 \cdot 10^{-4} \cdot \text{FREQ} - 5.704 \cdot 10^{-8} \cdot \text{FREQ} \cdot \text{NEEV} \quad (1)$$

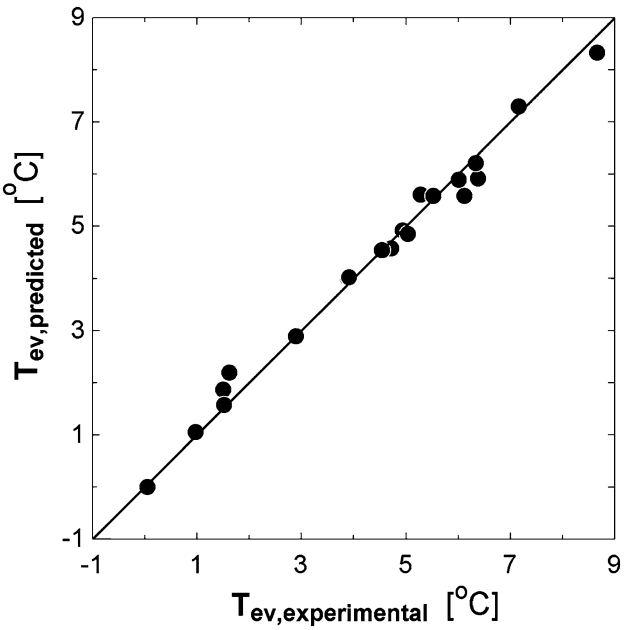

Fig. 3 Comparison between experimental values of the evaporating temperature and those predicted by the model, Eq. (2)

$$T_{ev} = 18.178 + 0.00427 \cdot \text{NEEV} - 4.207 \cdot 10^{-6} \cdot \text{NEEV}^2 - 0.2718 \cdot \text{FREQ} \quad (2)$$

The use of the surface design methodology allows for a relatively precise determination of the refrigerant flow rate and the evaporation temperature as a function of NEEV and FREQ, as shown in Fig. 2a, b, respectively. The objective function, Eqs. (1) and (2), obtained experimentally, describes the behaviour of the refrigerant flow rate as a function of compressor frequency, FREQ, and the number of steps of the electronic expansion valve, NEEV. Figure 3 shows the good agreement between experimental and predicted, Eq. (2) values of the evaporating temperature. This

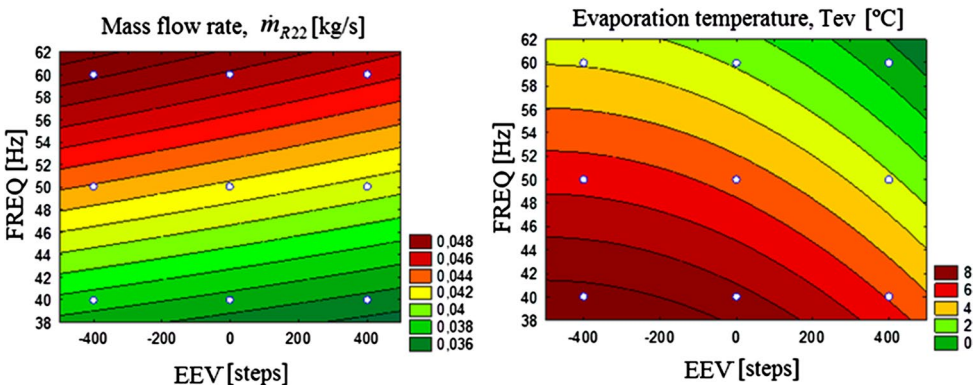

Fig. 2 Variation of refrigerant mass flow rate ($\dot{m}_{R22}$) and evaporation temperature (T_{ev}) with compressor frequency and steps of the electronic expansion valve

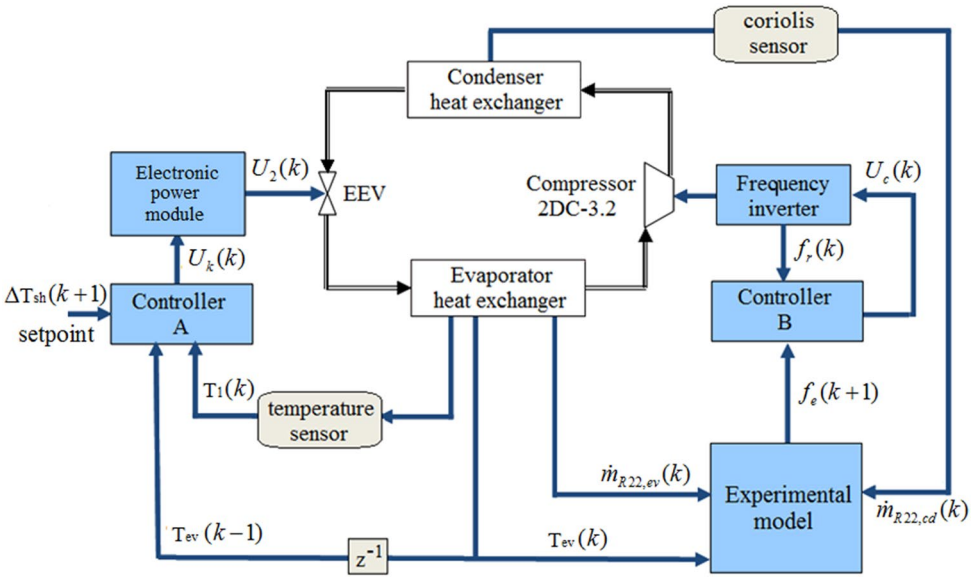

Fig. 4 Schematic view of a closed loop control system using the experimental model

was an expected outcome since the model is clearly an equation that fits experimental data.

The degree of superheating was adjusted by the proposed fuzzy adaptive control, by means of experimental tuning. The steady-state behaviour, Eqs. (1) and (2), was used as the starting point.

Figure 2a shows that the refrigerant mass flow rate is significantly controlled by FREQ and presents little dependency on EEV. On the other hand, Fig. 2b shows that the evaporation temperature is affected by both FREQ and EEV.

The two objective functions, refrigerant mass flow rate and evaporation temperature, Eqs. (1) and (2), form a mathematical model composed by non-linear algebraic equations which can be solved by a Labview software built-in solver, thus allowing for the estimate of the quasi dynamic behaviour of the compressor. Therefore, the purpose of the experimental model is to predict other time-dependent outputs of the system and also to facilitate the implementation of future actions so as to maintain the system close to a stable reference. The control algorithm was obtained experimentally, following the trajectory criteria, always searching for higher COP values. This was reached by guiding the trajectory through maximum values of the heat exchangers´ conductances (UA). The UA trajectory was calculated by means of a Labview subroutine (Simplex method), based on the prescribed evaporation and air temperatures. The controller optimizes the trajectory up to the desired evaporation temperature, while maintaining high UA values and improving the temperature difference at the evaporator outlet, thus ensuring a smooth variation of the evaporating temperature. Figure 4 shows the schematics of a closed loop control system using the experimental model of the system.

4 Implementation of adaptive fuzzy hybrid controls (PI, PID)

Two control schemes, A and B, were developed: control A is related to the number of steps of the electronic expansion valve and B, to the compressor speed. In relation to the compressor speed, the fuzzy adaptive control was used instead, since the controlled variables are more sensitive to it. In case of the control for the electronic expansion valve, the PI control was applied, to obtain the prescribed value of the degree of superheat. They are detailed below.

4.1 Control (A): fuzzy control of the degree of superheating

Control (A) is based on the architecture of a conventional proportional integrative (PI) fuzzy controller, used to control the stepper motor of the electronic expansion valve (EEV), as shown in Fig. 5.

The proposed control is tuned experimentally, with the following inputs: error and accumulated error in relation to the reference signal. The control is a result of the output signal (U_k) of the fuzzy controller multiplied by the gain (k_{pc}), introduced in the computer program, developed for the Labview platform, initially set equal to 1. The output signal to the actuator (U_2) generates a value (number of steps) that acts directly on the valve stepper motor.

Seven triangular fuzzy sets were used for each of the input variables. These sets are shown in Fig. 6, where each membership function is represented by an alphanumeric value: LN, MN, SN, ZO, SP, MP, LP, that mean large negative, medium negative, small negative, zero, small positive,

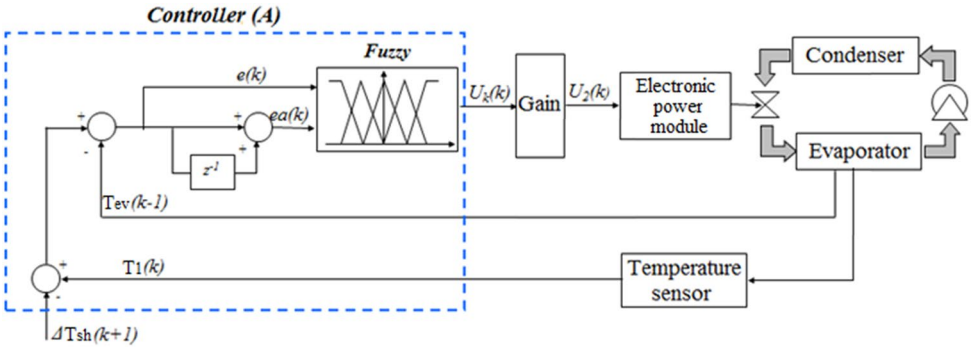

Fig. 5 Proposed fuzzy controller A for the electronic expansion valve

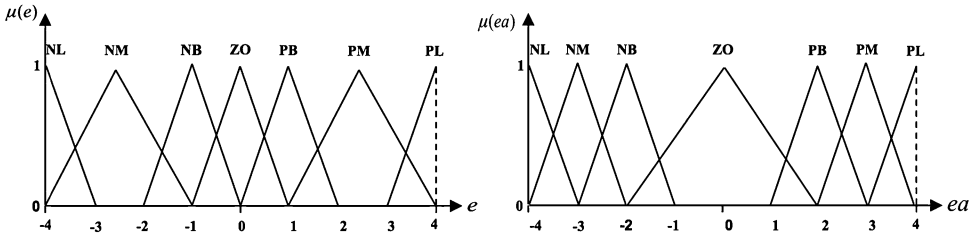

Fig. 6 Triangular fuzzy sets were used for each of the input variables, namely, error (e) and accumulated error (ea)

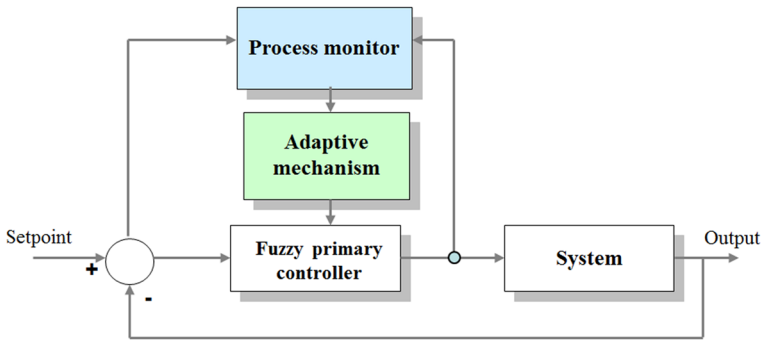

Fig. 7 Components of the adaptive fuzzy controller (B)

medium positive, and large positive, respectively. The universe of discourse for the error and accumulated error of the variables is defined as [−4, 4]. The inference mechanism selected was the max-product and the output zero-order Sugeno model, according to Takagi and Sugeno [25], with values LN = −8, MN = −4, SN = −2, ZO = 0, SP = 2, MP = 4, LP = 8 for the output variable (U_k) defined in the interval [−8, 8] steps.

4.2 Control (B): adaptive fuzzy control of compressor motor speed

This control is based on an adaptive fuzzy logic to control the frequency of the compressor. The relevance of this type of adaptive controller, unlike conventional fuzzy controllers, is its automatic adjustment to adapt to new characteristics of the process under control [3]. In order to identify the changes and to adapt to new conditions, two additional components were added, as shown in Fig. 7. The first component is the "Process Monitor", which detects changes in process characteristics, such as the yield performance of the controller or a parameter based on the behaviour of the process. The second additional component is the "adaptive mechanism" which, based on information from the process monitor, updates the controller parameters such as scale factor of each controlled variable, fuzzy set of alphanumeric variables or knowledge base rules.

For each of these inputs three membership functions [(N) negative, (Z) zero and (P) positive] were defined. The functions are triangular, equally spaced and set within a universe of discourse tuned heuristically. The output of the fuzzy controller is a zero-order Sugeno model with constant values ($N = 1.0$, $Z = 0$ and $R = 1.0$) constant. For the adaptation mechanism, coupled to the primary fuzzy controller, a universe of discourse in a normalized interval [−1, 1] was established. The system was monitored based on the mean absolute change of the inlet error ($|\Delta\bar{e}|$) and the mean

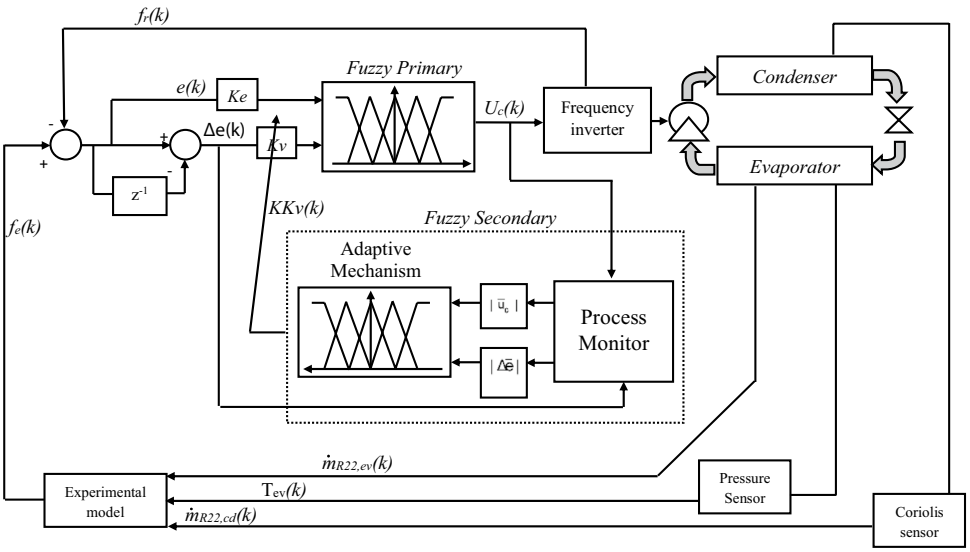

Fig. 8 Adaptive fuzzy controller B proposed to control the frequency of the compressor

absolute control output ($|\bar{U}c|$), using the last three sampling times.

Similarly, for each input of the fuzzy adaptation mechanism, three triangular membership functions [(S) small, (M) medium, and (L) large], equally spaced within the defined universe of discourse of input of the controlled variables tuned heuristically, were defined. The inference mechanism selected was the max-product and the output zero-order Sugeno model. It can be varied by ±20%.

To control the frequency of the compressor, based on the information above, a primary fuzzy controller and, subsequently, a fuzzy adaption mechanism of the gains, were initially implemented as shown in Fig. 8. The input variables of the fuzzy controller were evaluated from the signals of the error $e(k)$ and the error variation $\Delta e(k)$, where $f_e(k)$ is the estimated frequency and $f_r(k)$ is the real frequency.

In general, the purpose for the control of compressor speed is to maintain constant the evaporation temperature. One of the consequences, in the present case, is related to the reduction in energy consumption.

5 Experimental procedure

As mentioned before, the experiments were conducted based on the response surface methodology, the central composite design of experiments and the Box–Behnken design. A face-centred central composite design (FCCCD) using two main parameters, such as, NVEE and FREQ, was adopted. Under these conditions, nine test runs were carried out. The first four runs used the experimental model of the system, Eqs. (1) and (2). For the first two runs, a degree of superheat of 7 °C was established as the set point and, for the others two, 2 °C. The next four runs, fifth to eighth, used the compressor map model obtained from the manufacturer and the set point was the same as explained before. The ninth run used the model of the system with trajectory optimization and a degree of superheating of 7.5 °C was established as the set point. It is important to highlight that initial conditions were different, although the thermal load was the same for all runs of tests.

The system was started up with the controller operating in closed loop and was monitored until steady state was reached, by regulating simultaneously the position of the expansion valve and the compressor frequency, while maintaining the prescribed degree of superheating. This procedure, in general, took at least 45 min for each test.

6 Results and discussion

Table 3 presents an overview of all experimental runs conducted in the present study. As mentioned before, the control structure showed its viability according to the accommodation time (t_a) to search the specified set point of degree of superheating, 7 and 2 °C, respectively.

Figures 9, 10, 11, 12 and 13 present results from the first run, which are detailed next. The test was initiated with the compressor frequency at 60 Hz (1750 rpm), an evaporation temperature of −11.8 °C and a degree of superheating of 27.1 °C. The thermal load was imposed upon the system with the evaporator inlet water temperature at 20 °C and mass flow rate 0.23 kg/s. For the heat removal at the condenser, the water flow rate was set at 0.989 kg/s.

After operating for 17 s in the transitional regime, the controller was activated to lead the system to a new steady state, as shown in Figs. 9, 10, 11, 12 and 13. The transition duration was approximately 218 s and a dead time of

Table 3 General characteristics of all experimental runs conducted in the present study

Battery	Initial condition	Final condition	Set point	t_a (s)	$\dot{Q}_{ev}$ (kW)	COP_{max}
B1	$f = 60$ Hz $T_{ev} = -11.8$ °C $\Delta T_{sh} = 27$ °C	$f = 30.5$ Hz $T_{ev} = 8$ °C $\Delta T_{sh} = 7.2$ °C	$\Delta T_{sh} = 7.0$ °C	218	6.42	3.0
B2	$f = 35$ Hz $T_{ev} = -9$ °C $\Delta T_{sh} = 26$ °C	$f = 32.4$ Hz $T_{ev} = 9.5$ °C $\Delta T_{sh} = 6.9$ °C	$\Delta T_{sh} = 7.0$ °C	181	6	3.0
B3	$f = 60$ Hz $T_{ev} = -11.5$ °C $\Delta T_{sh} = 23$ °C	$f = 31.7$ Hz $T_{ev} = 6$ °C $\Delta T_{sh} = 3.0$ °C	$\Delta T_{sh} = 2.0$ °C	130	6.82	3.1
B4	$f = 35$ Hz $T_{ev} = -9$ °C $\Delta T_{sh} = 24.9$ °C	$f = 32$ Hz $T_{ev} = 9$ °C $\Delta T_{sh} = 2.5$ °C	$\Delta T_{sh} = 2.0$ °C	122	6.23	3.1
B5	$f = 60$ Hz $T_{ev} = -10$ °C $\Delta T_{sh} = 24$ °C	$f = 40.2$ Hz $T_{ev} = 9$ °C $\Delta T_{sh} = 7.1$ °C	$\Delta T_{sh} = 7.0$ °C	131	6.92	3.1
B6	$f = 35$ Hz $T_{ev} = -12$ °C $\Delta T_{sh} = 30$ °C	$f = 40$ Hz $T_{ev} = 8.7$ °C $\Delta T_{sh} = 7.4$ °C	$\Delta T_{sh} = 7.0$ °C	80	6.15	2.8
B7	$f = 60$ Hz $T_{ev} = -14$ °C $\Delta T_{sh} = 27.8$ °C	$f = 42.3$ Hz $T_{ev} = 6$ °C $\Delta T_{sh} = 2$ °C	$\Delta T_{sh} = 2.0$ °C	152	7.12	3
B8	$f = 35$ Hz $T_{ev} = -9$ °C $\Delta T_{sh} = 25$ °C	$f = 46$ Hz $T_{ev} = 6$ °C $\Delta T_{sh} = 2.2$ °C	$\Delta T_{sh} = 2.0$ °C	160	7.1	2.83
B9	$f = 60$ Hz $T_{ev} = -11$ °C $\Delta T_{sh} = 23$ °C	$f = 39.6$ Hz $T_{ev} = 5$ °C $\Delta T_{sh} = 7.5$ °C	$\Delta T_{sh} = 7.5$ °C	265	6.9	3.1

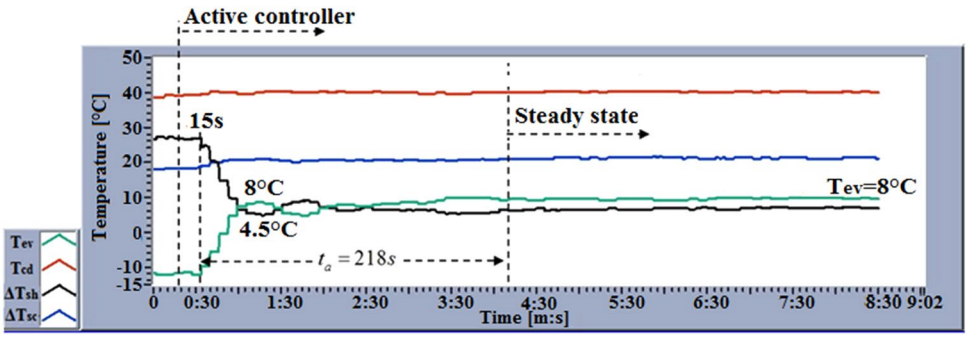

Fig. 9 Variation with time of condensing and evaporating temperatures and of degrees of superheating and subcooling during the first run

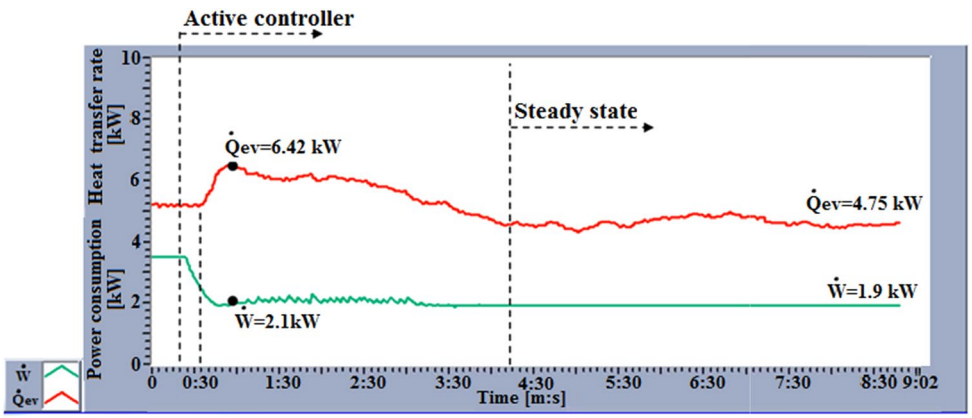

Fig. 10 Variation with time of cooling capacity and power consumption. Data obtained in the first run

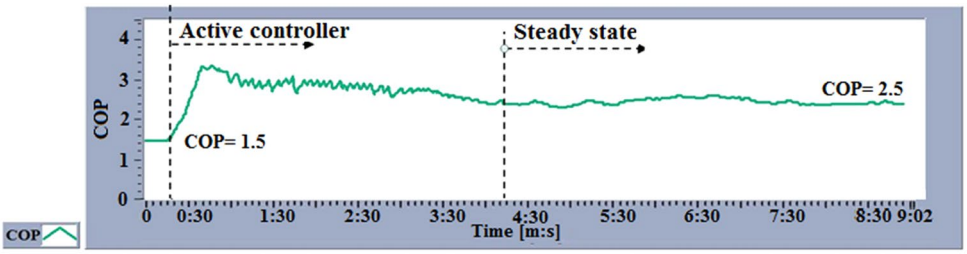

Fig. 11 Variation with time of coefficient of performance obtained during first run

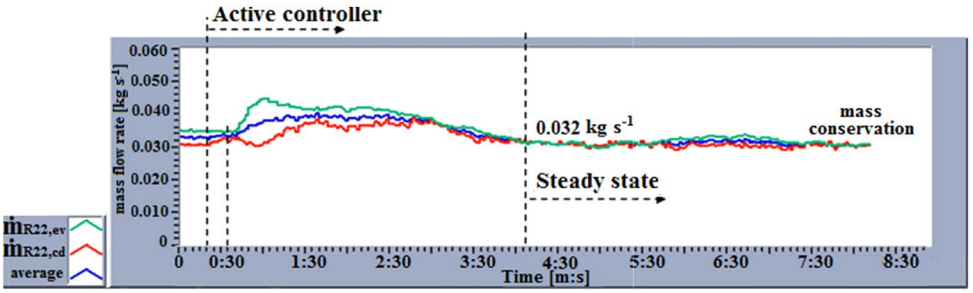

Fig. 12 Variation with time of refrigerant mass flow rate through the heat exchangers obtained during first run

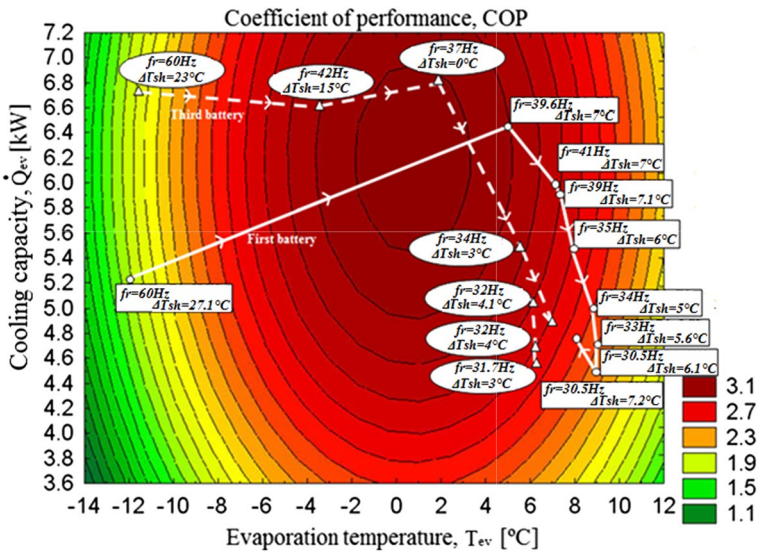

Fig. 13 Control trajectories for the coefficient of performance, compressor frequency and evaporator overall conductance as functions of the cooling capacity and the evaporation temperature, for the first and third runs

15 s was observed. The final degree of superheating was established in 7.0 °C. On the other hand, the final evaporation temperature and degree of subcooling were not prescribed.

In the first run of tests, the cooling capacity, $\dot{Q}_{ev}$, in Fig. 10, showed a decrease of 500 W during the test, from an initial condition of 5.25–4.75 kW, at steady state, with a final power consumption of 1.9 kW. The maximum value of $\dot{Q}_{ev}$, approximately 6.42 kW with a power consumption of 2.1 kW, occurred at 56 s. The variation of the coefficient of performance COP is shown in Fig. 11. The controller improved the coefficient of performance of the system during its operation, from 1.5 to 2.5. It can be seen, in Fig. 11, that the proposed control strategy always operates in higher COP values. In this case, the control system acted simultaneously in the electronic expansion valve and the compressor speed. It is also important to observe that, if the controller acted in the compressor velocity alone, the power consumption would increase substantially.

Figure 12 shows the evolution of the refrigerant mass flow rate through the heat exchangers, 0.032 kg/s, confirming the equalization of mass flow rate throughout the cycle, when steady state is reached, from about 250 s.

Figure 13 shows the COP as a function of cooling capacity, $\dot{Q}_{ev}$, and evaporation temperature, T_{ev}, for the first and third runs. They started with an initial degree of superheating of 23.0 and 27.1 °C, respectively, and a compressor

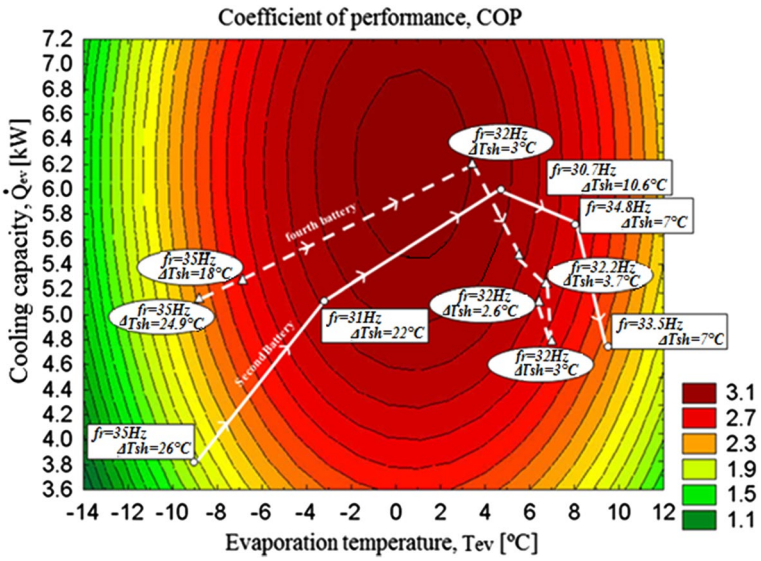

Fig. 14 Control trajectories for the coefficient of performance, compressor frequency and evaporator overall conductance as functions of the cooling capacity and the evaporation temperature, for the second and fourth runs

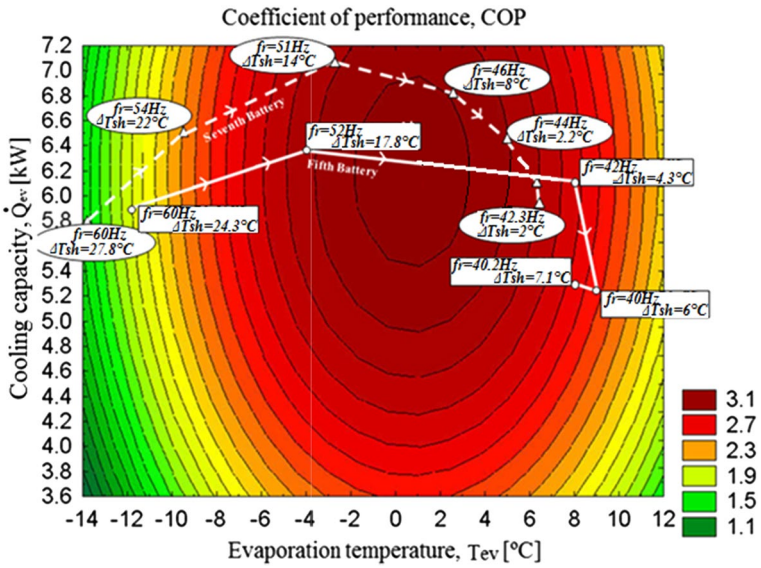

Fig. 15 Control trajectories for the coefficient of performance, compressor frequency and evaporator overall conductance as functions of the cooling capacity and the evaporation temperature, for the fifth and seventh runs

frequency of 60 Hz. Figure 13 helps synthesize and better understand the behaviour and effect of the hybrid controller in search for the desired final state. Note that the trajectory for the third run (dashed line), with a minimum prescribed degree of superheating of 2 °C, passed through regions of high value of COP without major oscillations. This effect is due to the influence of the controller gain (k_{pc}) setting of controller (A), which acts on the expansion valve according to the system dynamics.

The same comparison was conducted for the second and fourth runs, Fig. 14, with an initial degree of superheating of 26 and 24.9 °C, respectively, and an initial compressor frequency of 35 Hz. The trajectory of the fourth run achieved the highest COP. In both runs, the oscillations in transient regime were minimized and settled in a working range between 32 and 35 Hz. The system dynamics presented a more damped behaviour during these two runs. A short convergence time was achieved in the fourth run, adjusting correctly the degree of superheating. It can be stated that such conditions led to promising results for refrigeration systems, operating with hybrid adaptive fuzzy controlled systems, working simultaneously on their controlling variables.

In the fifth and sixth runs the final degree of superheating was 7 °C, whereas for the seventh and eighth runs, 2 °C.

Figure 15 shows that, in comparison with the trajectory of the fifth run (continuous line), that of the seventh run (dashed line—minimum degree of superheating of 2 °C) resulted in straightforward COP improvement. This is

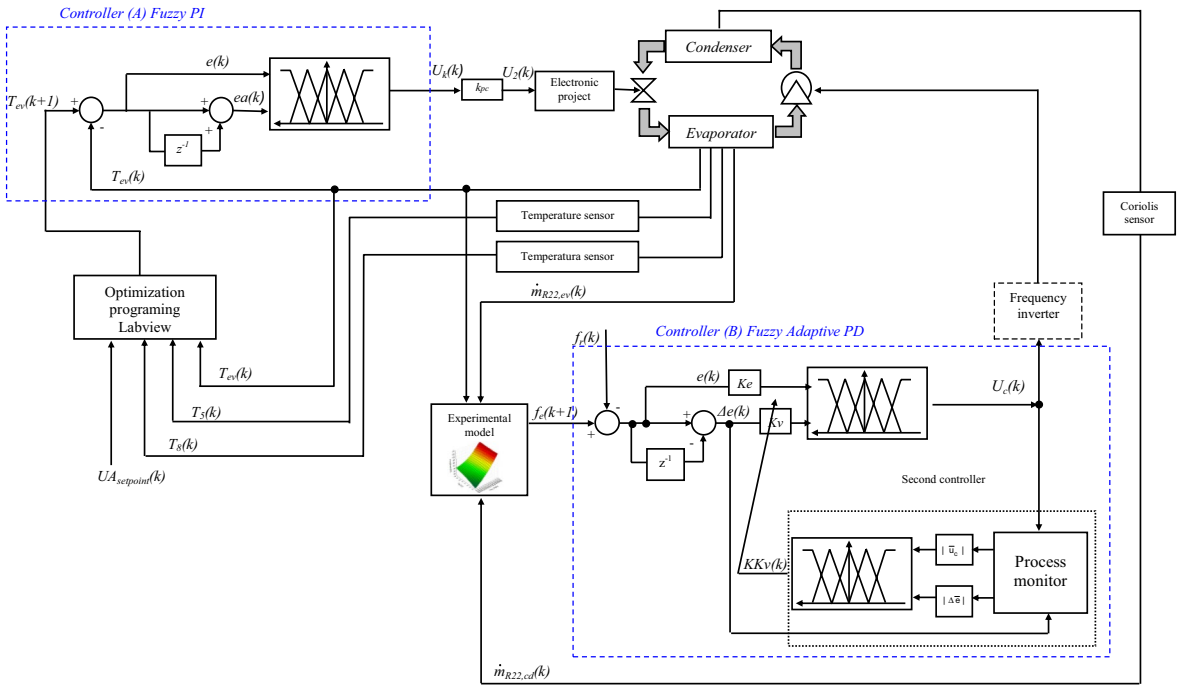

Fig. 16 Scheme of the trajectory control of the hybrid fuzzy adaptive controller

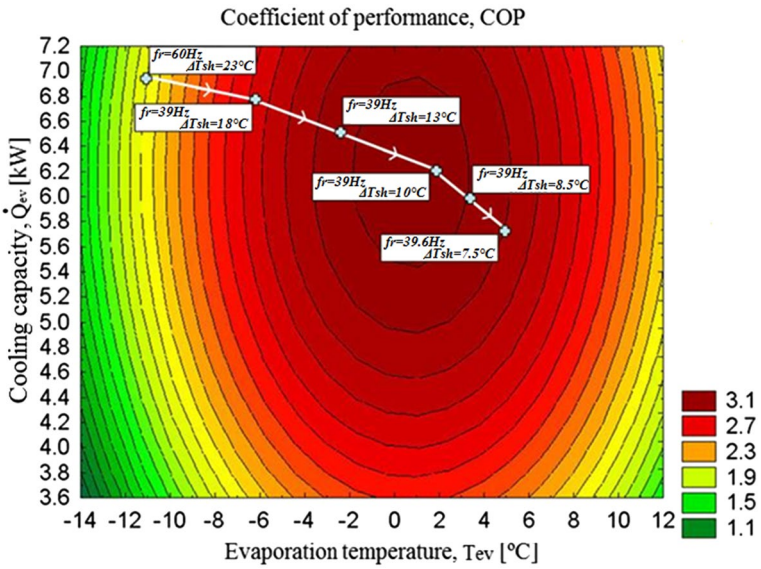

Fig. 17 Behavior of the control trajectory of the hybrid fuzzy adaptive controller for the coefficient of performance as a function of the cooling capacity and evaporation temperature

probably due to the influence of gain setting k_{pc} of controller (A) and working mode of medium steps acting on the expansion valve, leaving the controller with a finer adjustment, more appropriate for this type of system.

Runs (B3) and (B4) worked with the system model and controlled the minimum degree of superheating in 2 °C. The adjustment in internal gain, $k_{pc} = 0.5$ in the program, is a way to offset the influence of the controller response output to the expansion valve. This enabled a good overall result, run (B3), demonstrated by the performance indices, ITAE equal to 750, and IAE, 21, if compared with run (B1), which had 1400 and 22.5, respectively. This comparison was made possible as runs (B3) and (B1) started with the same initial conditions, of compressor frequency of 60 Hz. Likewise, run (B4) showed lower index values (ITAE = 250 and IAE = 29) if comparison is made with run (B2), under the same initial conditions of for compressor frequency of 35 Hz.

The performance indices for runs (B7) and (B8), with the compressor model, were influenced by the excessive

Table 4 Comparison of the average coefficient of performance, COP, obtained with different control strategies used in the present work

Control	COP
On–off	1.99
Adaptive fuzzy	2.43
Hybrid fuzzy—compressor model	2.52
Adaptive—experimental model	2.68
Hybrid fuzzy—trajectory optimization	3.03

contribution of the error of the variable in the beginning of the run. This is due to the response of the expansion valve being set to medium step mode. However, the objective to control the degree of superheating at around 2 °C was achieved, but with higher settling times, if compared to runs (B3) and (B4).

Figure 16 shows the control scheme for use of the model of the cooling system and controlled trajectory. The highest values of average COP were obtained by guiding the trajectory to obtain the maximum values of the heat exchanger conductances (UA), without peaks in cooling capacity. During these tests, the search for minimum degree of superheating was possible; however, with a greater transition time, jeopardizing a rapid response of the controller. It is interesting to note that, in Fig. 17, maximum values of COP were obtained, where the controller optimized the trajectory through regions of higher overall heat transfer coefficients, without stand time and maximum peaks in the cooling capacity.

The hybrid adaptive fuzzy control, with optimized trajectory (B9), as shown in Fig. 17, had the highest values of COP during transient operation of the control, resulting in an average COP of 3.03. Table 4 shows the values of the average coefficients of performance (COP) obtained with the different control strategies tested in this work.

7 Conclusions

A 5-ton vapour compression system with a variable speed compressor and an electronic expansion valve was constructed to evaluate the thermal performance of the system by the use of adaptive fuzzy hybrid control. The methodology used in the design of experiments of this study allowed an objective and simple way to know the dynamics of the system and its controller. The change in frequency of the compressor resulted in significant changes in the evaporation temperature. The same was observed when acting on the opening and closing of the expansion valve, confirming the adequacy of these parameters as variables for controller designs.

In this work, a model for controlling the degree of superheating with good stability, exploiting the advantage of fuzzy controllers, was developed. The hybrid adaptive fuzzy control, here developed, was a reasonably efficient method to achieve the best average COP in dynamic operation of the system, taking into account the high level of overall conductance of the evaporator, UA. By imposing the dynamic path of the controller, the proposed system was able to adjust the degree of superheating, by means of operation via surfaces with high COP using low rotation frequencies (35 and 40 Hz). One important point distinguishes the controller proposed here from others: it works based on the response to the overall heat transfer coefficient, which makes the system operate alongside zones of high COP (as the evaporator remains flooded for most of the time). Conventional controllers do not take that into account, as they simply actuate in the compressor and the expansion valve, following the cooling demand.

Finally, it is important to highlight that the authors recommend the fuzzy hybrid control technique, based on the UA parameter, since it has been found to be one of the most efficient of the tested group, in addition to contributing to a significant overall energy conservation.

Acknowledgments The authors gratefully acknowledge the support of CNPq, CAPES, FAPERJ and FAPEMIG.

References

1. Abernethy RB, Thompson JW (1980) Handbook: uncertainty in gas turbine measurements. Va. National Technical Information Service, Springfield
2. Aprea C, Mastrullo R, Renno C (2008) Fuzzy control of the compressor speed in a refrigeration plant. Int J Refrig 27(6):639–648
3. Bandarra Filho EP, Garcia FEM, Mendoza OSH (2011) Application of adaptive control in a refrigeration system to improve performance. J Braz Soc Mech Sci Eng 33:21–30
4. Box GEP, Draper NR (1987) Empirical model-building and response surfaces. John Wiley & Sons, New York
5. Box GEP, Hunter JS, Hunter WG (2005) Statistics for experimenters, 2nd edn. Wiley, New York
6. Chen W, Zhijiu C, Ruiqi Z, Yezheng W (2002) Experimental investigation of a minimum stable superheat control system of an evaporator. Int J Refrig 25(8):1137–1142
7. Dhar M, Soedel W (1979) Transient analysis of vapor compression refrigeration system: part I, mathematical model and part II, computer simulation. In: Proceedings of 15th international congress of refrigeration meeting Venice, Italy, pp 1035–1067
8. Dossat RJ, Horan TJ (2001) Principles of refrigeration, 5th edn. Wiley, Hoboken, NJ
9. Ekren O, Kucuka S (2010) Energy saving potential of chiller system with fuzzy logic control. Int J Energy Res 34(10):897–906
10. Ekren O, Sahin S, Isler Y (2010) Comparison of different controllers for variable speed compressor and electronic expansion valve. Int J Refrig 33:1161–1168
11. Higuchi K, Hayano M (1982) Dynamic characteristics of thermostatic expansion valves. Int J Refrig 5(4):216–220

12. Jia X, Tso CP, Chia PK (1995) A distributed model for prediction of the transient response of an evaporator. Int J Refrig 18(5):336–342
13. Jian-peng C, Jeong S, Jung Y (2014) Fuzzy logic controller design with unevenly-distributed membership function for high performance chamber cooling system. J Cent South Univ 7:2684–2692
14. Koury RNN, Machado L, Ismail KAR (2001) Numerical simulation of a variable speed refrigeration. Int J Refrig 24:192–200
15. Lenger MG, Jacobi AM, Hrnjak PS (1998) Superheat stability of an evaporator and thermostatic expansion valve. Air Conditioning and Refrigeration Center, University of Illinois Mechanical and Industrial Engineering Department, report ACRC TR-138, 1206 West Green Street, Urbana, IL 61801(217):333–3115
16. Marcinichen JB, Schurt LC, Melo C, Vieira LAT (2008) Performance evaluation of a plug-in refrigeration system running under the simultaneous control of compressor speed and expansion valve opening. 12th International Refrigeration and Air Conditioning Conference at Purdue
17. Mithraratne P, Wijeysundera NE (2002) An experimental and numerical study of hunting in thermostatic-expansion-valve-controlled evaporators. Int J Refrig 25(7):992–998
18. Myers RH, Montgomery DC (1995) Response surface methodology: process and product optimization using designed experiments. John Wiley & Sons, New York, NY
19. Oliveira V, Trofino Neto A, Hermes CJL (2011) A switching control strategy for vapor compression refrigeration systems. Appl Therm Eng 31:3914–3921
20. Outtagarts A, Haberschill P, Lallemand M (1995) Comportement dynamique d'un évaporateur de machine frigorifique soumis a` des variations de debit. In: Proceedings of 19th international congress of refrigeration, B2. La Haye, pp 413–420
21. Pinolla CF, Vargas JVC, Buiar CL, Ordonez JC (2015) Energy consumption reduction in existing HVAC-R systems via a power law controlling kit. Appl Therm Eng 82:341–350
22. Rajendran H, Pate M (1986) A computer model of the start-up transients in a vapor compression refrigeration system. In: International refrigeration and air conditioning conference, Paper 17. http://docs.lib.purdue.edu/iracc/17
23. Shunagquan S (2004) Performance representation of variable-speed compressor for inverter air conditioners based on experimental data. Int J Refrig 27:805–815
24. Schurt LC, Hermes CJL, Trofino-Neto A (2009) A model-driven multivariable controller for vapor compression refrigeration systems. Int J Refrig 32:1672–1682
25. Takagi T, Sugeno M (1985) Fuzzy identification of systems and its applications to modeling and control. IEEE Trans Syst Man-Cybern 15(1):116–132
26. Tsai C, Tsai K, Su C (2012) Cascaded fuzzy-PID control using PSO-EP algorithm for air source heat pumps. In: International conference on fuzzy theory and its applications (iFUZZY), Taichung, 16–18 Nov 2012
27. Vargas JVC, Parise JAR (1995) Simulation in transient regime of a heat pump with closed-loop and on-off control. Int J Refrig 18(4):235–243
28. Yasuda H (1994) Modeling of refrigeration cycle dynamics for air conditioner. Trans JSME 60(573):103–110